Analysis of the polarized IR reflectance spectra of the monoclinic α-oxalic acid dihydrate

[1]Vladimir Ivanovski, [2,3]Thomas G. Mayerhöfer, [4]Jernej Stare, [4]Marta Klanjšek Gunde*, and [4]Jože Grdadolnik*

[1]*Institute of Chemistry, Faculty of Natural Sciences and Mathematics, Ss. Cyril and Methodius University in Skopje, Arhimedova 5, 1000 Skopje, Republic of Macedonia*

[2]*Leibniz Institute of Photonic Technology (IPHT), Albert-Einstein-Str. 9, D-07745 Jena, Germany*

[3]*Institute of Physical Chemistry and Abbe Center of Photonics, Friedrich Schiller University, Jena, D-07743, Helmholtzweg 4, Germany*

[4]*National Institute of Chemistry, Hajdrihova 19, SI-1000 Ljubljana, Slovenia*

Abstract

In contrast to the extensive molecular and crystal structure investigations on oxalic acid dihydrate ($C_2H_2O_4 \cdot 2H_2O$, α-POX) and its deuterated analogues (α-DOX), stands the absence of a complete vibrational spectra analysis. Such analysis is desirable in view of the proton dynamics in α-POX crystals. In this communication we report the room temperature polarized IR reflectance spectra of a single crystal of α-POX recorded from the *ac* crystal plane, and from the plane containing the *b*-crystallographic axis, with polarization along the axis. Dispersion analysis of the reflectance spectra of both B_u and A_u symmetry type modes, using model dielectric and reflectance function valid for the monoclinic case, have been performed and the results are discussed. Some aspects of the obtained fit results for some of the spectral regions and the peculiar change of the reflectance function with polarization angle are also discussed in this work. A correlation between the crystal structure and measured spectra, together with the results of the performed dispersion analysis, gave answers to some of the problems concerned with the orientation of the transition dipole moments of the IR active modes. The assignment of modes is assisted by DFT calculations. Another aspect covered in this work is the model reflectance functions using different averaging theories that have been applied in obtaining the reflectance spectrum of a polycrystalline sample. The results of the comparison between these spectra and the recorded reflectance spectra from a polycrystalline sample were further discussed.

*corresponding authors: **joze.grdadolnik@ki.si.**

marta.k.gunde@ki.si.

1. Introduction

The interest towards investigation of oxalic acid dihydrate ($C_2H_2O_4 \cdot 2H_2O$, α-POX) appeared due to its peculiar properties arising from the existence of a very short hydrogen bonds in its structure [1, 2]. It has been shown [3] that a proton transfer between the O–H acid group and the short hydrogen bonded water molecules at 17 °C, occurs at ms time-scale. The ac conductivity in the α-POX crystals as a function of the temperature and the applied frequency has also been investigated [4]. One of the conclusions of that work is that at temperatures below 200 K, proton polarons are involved in the conductivity. Some preliminary results have shown that these polarons may be the reason for an observed intensity enhancement in the region around 1400 cm^{-1} in the IR and Raman spectrum of the crystal of oxalic acid dihydrate [4, 5], as compared to the crystals of acetanilide [6] and methyl acetamide [7]. All these peculiarities result in a necessity for accurate vibrational characteristics of α-POX crystals. Although complete crystal structure investigations of α-POX [1, 2], its deuterated analogue ($C_2D_2O_4 \cdot 2D_2O$, α-DOX) [2] and the β polymorph (β-DOX) [8, 9] exist, the crystal dynamics picture is still not complete. At first sight it seems due to a comparably small number of atoms in the formula unit and a small number of formula units per primitive cell ($Z = 2$), IR and Raman spectra of α-POX should be easy to interpret. But, on the contrary, in the few existent investigations [5, 10-12] of the vibrational properties of α-POX, it has been shown that the interpretation of the vibrational spectra is far from being straightforward.

The crystal structure investigations reveal that all of the polymorphs are monoclinic (the space group is $P2_1/n$ for α and $P2_1/a$ for β polymorph). In both structures a center of inversion is present imposing the exclusion rule. Thus A_u and B_u symmetry type modes are IR active, while A_g and B_g are Raman active only. A complete picture of the vibrational dynamics of the crystal can be obtained only if both types of spectra are collected. Recently, a complete polarized Raman investigation on α polymorph has been published [11]. To obtain the complementary IR data it is necessary to study a single crystal by recording reflectance spectra with polarized light and interpreting this spectra by applying classical dispersion theory [13, 14], which satisfactory determines the mode parameters like transversal phonon frequencies, transition moment strengths, damping constants, and direction of transition dipole moment of the corresponding modes. According to the monoclinic crystal system in which α-POX crystallizes, we have applied a methodology suitable for this case, which already gave excellent results in previous studies on similar systems [15-17].

2. Experimental

Single crystals of α-POX were obtained from a concentrated water solution by slow evaporation. Crystals of different morphology resulted from this procedure: some of the obtained single crystals were needle shaped, while others resembled plate prisms. For the needle shaped crystals, X-ray diffraction measurements revealed that the *b* crystallographic axis lies along the needle axis, while in the case of plate prism crystals, the smallest developed plane was perpendicular to the *b* crystallographic axis. Crystallization at temperatures around 5 °C yields crystals of good quality but without preference of a certain morphology. Crystals grown at temperatures around 25 °C were of lower quality but with the morphology needed (plate like crystals). Because in none of the crystals the (010) crystal plane manifested itself in their macroscopic morphology, they were oriented in order to find the directions of the *a* and *c* crystallographic axes using XRD. The direction of the *b* axis was further assured recording an IR cross polarization spectrum where a zero cross polarization indicates perfect orientation in this case.

After orientation of the crystals, they were cut and polished. It has to be stressed that due to the organic nature of α-POX it was quite difficult to find a suitable non dissolving polishing agent being also a cooling agent during the polishing procedure. It appeared that polishing without a polishing agent induces structural changes on the crystal surface, monitored by the IR spectra. We finally decided to apply CCl_4, a non-polar and strong evaporating liquid that enables cooling during the polishing process. The polished planes were not of equal optical quality which reflects in the quality of reflectance spectra. Another challenge connected to the recording of the α-POX crystals was the loss of crystal water. Dehydration occurred particularly on freshly polished planes, especially when recording in dry atmosphere was performed. Therefore we strictly recorded the reflectance spectra in the presence of humid air, although the presence of water vapor and CO_2 bands slightly disturbed the spectral quality.

Infrared reflection spectra were recorded on Bruker Equinox 55 at room temperature. 64 scans were recorded at nominal resolution of 4 cm^{-1} and averaged. For spectra recorded with variation of the polarization angle in the *ac* plane, performed every 10°, a Fixed Angle Specular Reflectance Accessory at 8° incidence angle was employed. Spectra further applied in the fitting procedure were recorded using a Harrick-Scientific Seagull™ Reflectance Cell at 5° incidence angle. In both cases only s-polarized radiation was employed. The approximate dimension of the aperture used was between 3 and 4 mm. A face parallel to the *b*

crystallographic axis was also polished and spectra were recorded with polarization direction of the external radiation along this axis.

3. Computational approach

Harmonic vibrational analysis of the crystalline α-POX was performed on a previously minimized structure by using the plane-wave/Density Functional Theory (DFT) approach, as implemented in the CPMD v. 3.13.2 program package [18]. All the symmetry features of the system, including translational periodicity and space group operations, were rigorously followed. We used the BLYP density functional coupled with the plane-wave basis set with a kinetic energy cut-off of 80 Ry. While valence electrons were treated explicitly, the core electrons were approximated with atomic pseudopotentials of Trouiller and Martins [19]. A $2 \times 4 \times 1$ Monkhorst-Pack mesh of k-points was used in the electron structure calculations. This approach is in essence similar to the previously published study of vibrational modes of oxalic acid dihydrate in the context of Raman spectroscopy [11].

4. Dispersion analysis – theory

The orientation of the crystal axes, the internal xyz and the external XYZ coordinate systems are presented in Figure 1.
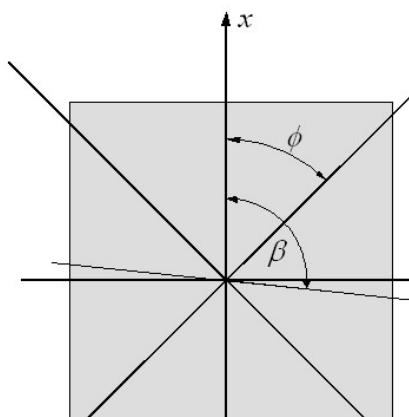
Figure 1. Measurement geometry applied for B_u spectra as viewed along b crystal axis, ($\beta = 106°20'$). Coordinate system fixed to the crystal is denoted by x, y, z and the system fixed to the polarization vector X of the external electric field vector by X, Y, Z.

From the given direction of rotation of the vector of polarization (X axis) it follows that the rotation transformation of the dielectric tensor from internal $\widetilde{\varepsilon}_{x,z}$ into external $\widetilde{\varepsilon}_{X,Z}$ coordinates should have the following form,

$$\widetilde{\varepsilon}_{X,Z}(\phi) = \begin{pmatrix} \cos\phi & \sin\phi \\ -\sin\phi & \cos\phi \end{pmatrix} \begin{pmatrix} \widetilde{\varepsilon}_{xx} & \widetilde{\varepsilon}_{xz} \\ \widetilde{\varepsilon}_{xz} & \widetilde{\varepsilon}_{zz} \end{pmatrix} \begin{pmatrix} \cos\phi & -\sin\phi \\ \sin\phi & \cos\phi \end{pmatrix}, \tag{1}$$

where ϕ is the angle between the x and X coordinate axes, which coincides with the angle between the a crystallographic axis and the direction of polarization of the external radiation. The dielectric tensor in terms of the crystal fixed xyz coordinate system is expressed through the background tensor components $\varepsilon_{xx}{}^\infty$, $\varepsilon_{xz}{}^\infty$, $\varepsilon_{zz}{}^\infty$, oscillator strengths S_t^2, transversal phonon frequencies ω_t, attenuation constants γ_t and the orientation of the transition dipole moments θ_t, through the relation [15, 16].

$$\widetilde{\varepsilon}_{x,z} \equiv \begin{pmatrix} \widetilde{\varepsilon}_{xx} & \widetilde{\varepsilon}_{xz} \\ \widetilde{\varepsilon}_{xz} & \widetilde{\varepsilon}_{zz} \end{pmatrix} = \begin{pmatrix} \varepsilon_{xx}^\infty & \varepsilon_{xz}^\infty \\ \varepsilon_{xz}^\infty & \varepsilon_{zz}^\infty \end{pmatrix} + \sum_{k=1}^{N} \begin{pmatrix} \cos^2\theta_{tk} & \cos\theta_{tk}\sin\theta_{tk} \\ \cos\theta_{tk}\sin\theta_{tk} & \sin^2\theta_{tk} \end{pmatrix} \frac{S_{tk}^2}{\omega_{tk}^2 - \omega^2 - i\omega\gamma_{tk}} \tag{2}$$

In the summation, all transition dipole moments with vectors in the ac plane are involved. The reflectance function for reflections from the ac crystal plane at normal incidence is then calculated using the relation [13],

$$R_X(\phi) = \left|\widetilde{r}_{XX}\right|^2 + \left|\widetilde{r}_{XZ}\right|^2 , \tag{3}$$

where the $\widetilde{r}_{XX}$ and $\widetilde{r}_{XZ}$ are the complex reflectance amplitudes. The small incidence angle of $5°$ allowed us to use the simplified approach (using theory for normal incidence, on non-normal incidence reflectance data) as explained later in the text.

Much simpler formulas can be found elsewhere [20] for dielectric and reflectance functions of the optically isotropic case for reflection from a crystal plane parallel to the b crystal axis and polarization along this axis.

5. Results and discussion

Structural investigations of crystals of oxalic acid dihydrate show [1, 2] that two molecules of oxalic acid per primitive cell rest on sites with local symmetry i, while one set of four water molecules are on general positions, i.e. being on C_1 sites of symmetry. The correlation diagrams between the irreducible representations of point groups of a free oxalic acid and water molecules in a free state, the site symmetry in the crystal, and the factor group of the space group of the crystal, are presented in Figure 2. The diagram for oxalic acid presented below, is applied under the assumption of a C_{2h} point group symmetry of free oxalic acid molecule [21, 22].

$C_2H_2O_4$

C_{2v}	C_i	C_{2h}
$3A_u$	A_u	$9A_u$
$6B_u$		$9B_u$
$7A_g$	A_g	$9A_g$
$2B_g$		$9B_g$

H_2O

C_{2v}	C_1	C_{2h}
$2A_1$	A	$3A_u$
$1B_1$		$3B_u$
A_2		$3A_g$
B_2		$3B_g$
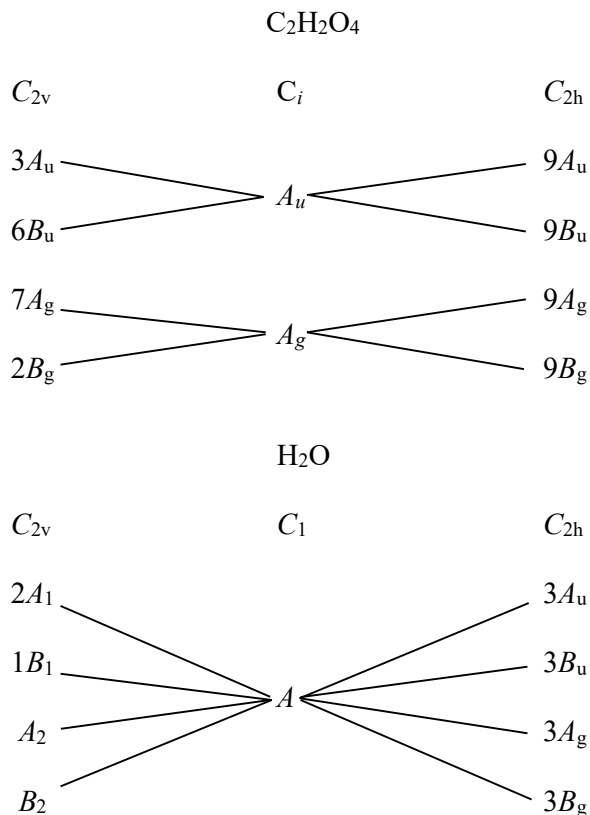
Figure 2. Correlation diagrams of oxalic acid and water molecule in the structure of α-POX

For free trans oxalic acid molecule, group theory gives the number of vibrations divided among the irreducible representation of the C_{2h} point group as, **$\Gamma_{\text{oxalic acid}}$ = 7 A_g ⊕ 2 B_g ⊕ 3 A_u ⊕ 6 B_u**. For the two molecules of oxalic acid, under the C_{2h} point group isomorphic with the space group, the symmetries of vibrations are **$\Gamma_{\text{oxalic acid in crystal}}$ = 9 A_g ⊕ 9 B_g ⊕ 9 A_u ⊕ 9 B_u**. The four water molecules in the primitive cell, will give 12 internal vibrations divided equally among the symmetry types. In contrast to oxalic acid, all of the vibrations present in the free water molecule will equally participate among the symmetry types characteristic for the crystal point group C_{2h}. For the oxalic acid, the modes will preserve the parity, so that some of the modes will exclusively be visible either in Raman or in IR spectra. For further analysis it is instructive to know the symmetry type of the internal and symmetry adapted coordinates for both the oxalic acid and water molecule. Therefore, we used the harmonic

6

frequencies and normal modes obtained from our DFT calculations. We apply only the ungerade (A_u and B_u) symmetry types when assigning the modes. Due to the appearance of a short hydrogen bond, which results in strong anharmonicity and coupling of particular modes, it is very difficult to distinguish between internal and external vibrations, so that the upper mode analysis is just an approximation.

In order to view the B_u symmetry type modes, the polarized IR reflectance spectra were recorded from the *ac* crystal plane, changing the direction of polarization by changing the angle ϕ (cf. Fig. 1) in the range from 0° to 180°, with a step of 10°. In order to obtain clearer picture only a part of the recorded spectra with a step in the change of the angle ϕ of 20° is presented in Figure 3. It is noticeable, that all bands change their intensity with respect to different orientations of the vector of polarization of the external radiation. Some bands have intensity minima close to zero, indicating that the transition dipole moment is oriented closely to the direction of the dielectric tensor of principal axes [23].
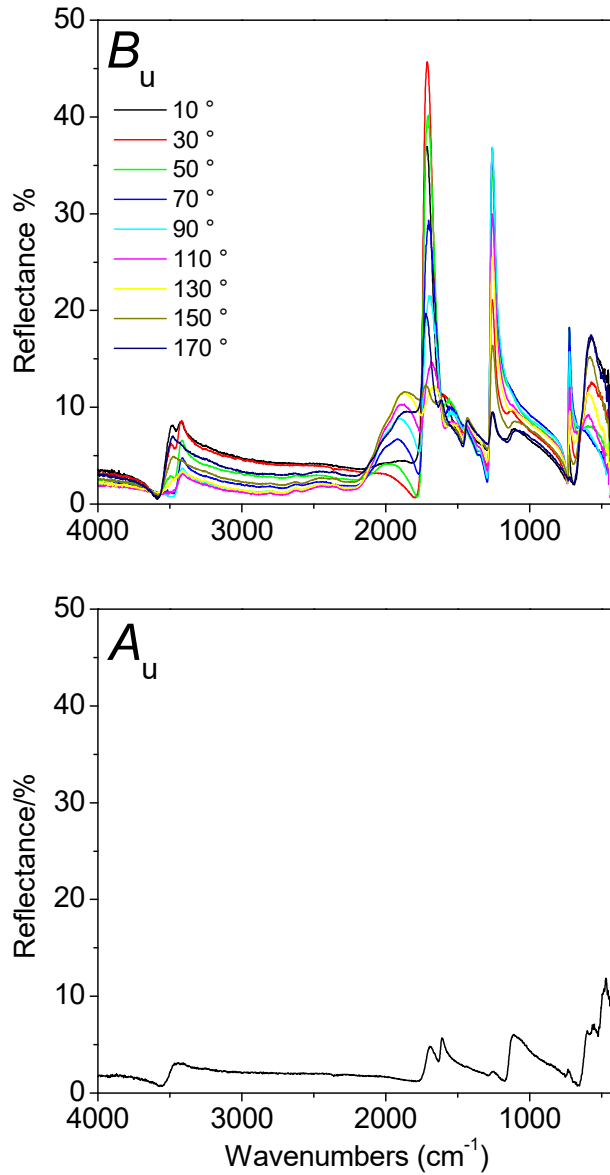
Figure 3. Reflectance spectra measured with the polarization vector perpendicular to *b* crystal axis (*ac* reflecting plane)-upper panel. The spectra were measured by rotating the crystal in the range between $0° < \phi < 180°$ by successive steps of 20°. The reflectance spectrum measured with polarization vector parallel to *b* crystal axis is presented in the lower panel.

In Figure 3, a spectrum recorded from the plane parallel to the *b* axis, with polarization along this axis is also presented. In this polarization, only modes of A_u symmetry are active. According to the correlation diagrams presented in Figure 2, the number of bands appearing in the spectra recorded from the *ac* crystal plane (B_u type) should be the same as ones which belong to A_u symmetry type. However, due to the unit cell group splitting, the frequencies differ. If the unit group splitting is small and can be neglected, then due to the different

8

projections of the transition dipole moment on the *ac* crystal plane and along the *b* crystallographic axis, the reflectance of the corresponding mode will also differ. Thus, comparing the change in the reflectance of the bands in the spectra recorded from the *ac* crystal plane, with the one recorded with polarization along the *b* crystal axis, following results for the "observed" orientations of the transition dipole moment (Table 1) can be obtained.

Table 1. Appearance of the most intense bands in the IR spectra applying different polarization of the external radiation.

	Wavenumber/cm^{-1}	3500	1891	1606	1540	1258	1116	723	473
Polariz.	along *a*			X	X				
	along *c*	X	X			X		X	
	along *b*	X		X			X		X

However, a visual observation of the band profile change in the polarized IR reflectance spectra with the change in the direction of polarization and conclusions about the directions of transition moments, can be safely done only for crystals with symmetry as high as orthorhombic. For monoclinic crystals, the transition dipole moments in the *ac* crystal plane are no longer fixed to unit cell symmetry. Therefore the direction of a transition dipole moment cannot be predicted from the symmetry considerations. Since the transition dipoles are usually not oriented along the directions of the crystallographic axes, the spectra are significantly more complex and consequently more challenging to interpret. Moreover, the number of reflectance bands, their positions and their shapes depend on the orientation of the vector of polarization.

The reflectance IR spectra of crystals crystallizing in monoclinic crystal system have been treated employing dispersion analysis [15-17, 24-26]. Four IR polarized reflectance spectra recorded from the *ac* crystal plane under incidence angle of 5° were used in the simultaneous fitting procedure presented in Figure 4. The low experimental incidence angle under which polarized spectra were recorded gave assurances that the obtained dispersion analysis results using the simple theory for normal incidence [24, 25] will not differ in a meaningful degree from the results employing the more complex theory that takes into account the incidence angle (averaged standard deviations of about 2% at 8° were obtained [26]). The modeled spectra arising from the best fit are also given for comparison, while the best fit parameter data are summarized in Table 2.
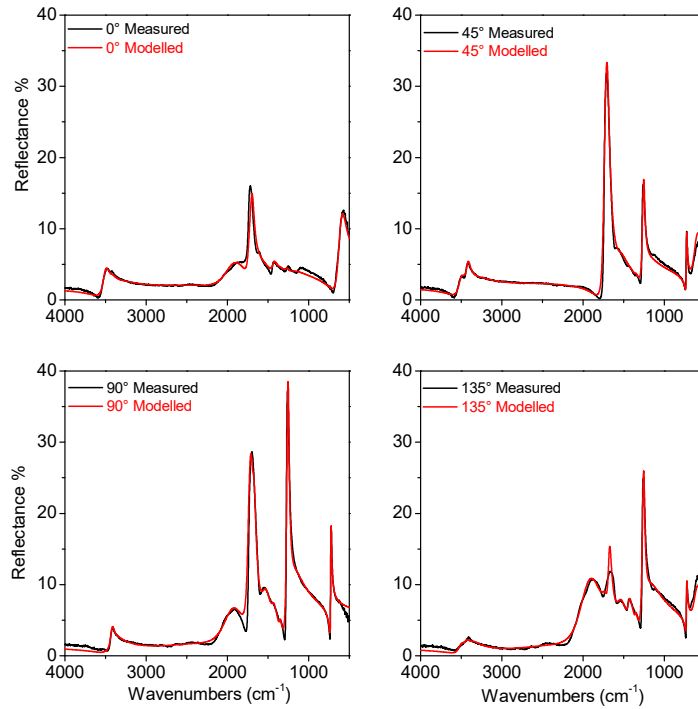
Figure 4. Polarized and modeled IR reflectance spectra recorded and calculated from the *ac* crystal plane at four angles ϕ: 0°, 45°, 90° and 135°.

Table 2. Parameters for the B_u symmetry type modes, obtained from the best fit of the polarized reflectance spectra recorded from the *ac* crystal plane. ω, S, γ and θ are: transversal frequency, square root of the oscillator strength S^2, damping constant, angle between the normal to the *c* crystallographic axis and the transition dipole moment direction of the B_u symmetry type mode, respectively. The observed frequencies (ω_{ob}) and the calculated ones applying the DFT approach (ω_c) are also given, together with the corresponding assignment.

α-POX (*ac*-plane)	ω_c/cm^{-1}	ω_{ob}/cm^{-1}	ω/cm^{-1}	S/cm^{-1}	γ/cm^{-1}	θ/°
ν(H_2O)	3463	3485	3498	562	104	10
ν(H_2O)	3389	3416	3416	370	58	67
			3369	427	170	111
			3299	377	283	36
combination		2799	2783	860	1837	27
combination		2622; 2463	2541	1169	1432	115
O–H---O_w stretching	1977	1883	1881	984	309	132

10

Assignment						
ν(C=O)+ δ(H_2O)		1720	1690	527	38	40
ν(C=O) + ν(C–O)+ δ(H_2O)	1634	1679	1667	506	45	92
ν(C=O) + ν(C–O)+ δ(H_2O)	1566	1541	1542	455	135	99
ν(C– O) + δ(C–O–H)	1451	1432	1432	247	64	133
ν(C– O) + γ(O – H)	1265	1351	1351	92	25	107
δ(O–H) + ν(C–O)	1239	1258	1247	438	19	95
γ(O – H)		1120	1188	554	214	108
O=C–O bend + O(3)H···O= out of plane bend	763	723	723	175	12	89
H_2O librations	554	573	590	368	102	3
$\varepsilon_{xx}(\infty) = 1.793$; $\varepsilon_{xz}(\infty) = 0.064$; $\varepsilon_{zz}(\infty) = 1.754$						

The fit was performed using 16 oscillators, according to the number of bands observed, which is less than predicted by the group theory. The addition of one or two extra oscillators did not significantly improve the similarity of modeled to recorded spectra. The reflectance spectra recorded along the b crystallographic axis, together with the modeled spectrum, using the data from the best fit, presented in Table 3, is presented in Figure 5.
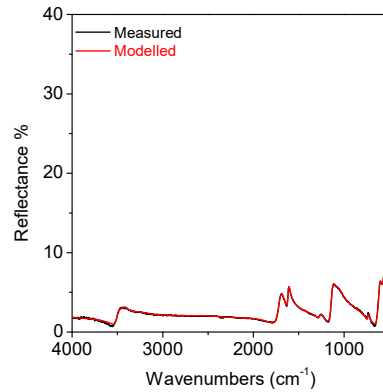
Figure 5. Polarized and modeled spectrum recorded and calculated from a plane parallel to the b crystal axis, with polarization along this axis.

Table 3. Parameters for the A_u symmetry type modes, obtained from the best fit of the polarized reflectance spectra recorded from the plane, parallel to the b crystallographic axis, with polarization of the incidence electric field along the axis. The designation of the parameters is the same as in Table 2.
* Assignment was taken from ref. [11].

α-POX ($\parallel$ b-axis)	ω_c/cm^{-1}	ω_{ob}/cm^{-1}	ω/cm^{-1}	S/cm^{-1}	γ/cm^{-1}

$\nu(H_2O)$	3457	3468	3492	336	73
$\nu(H_2O)$	3419	3424	3437	268	93
		3257	3301	213	183
combination		2628	2718	363	679
combination		2038	2010	372	643
$\nu(C=O)+ \delta(H_2O)$	1630	1690	1701	368	93
$\nu(C=O) + \nu(C-O)+ \delta(H_2O)$	1576	1608	1614	138	22
			1602	112	43
$\nu(C-O) + \delta(COH)$	1462	1439	1402	152	288
$\delta(COH) + \nu(C-O)$	1303	1254	1264	97	45
$\gamma(O-H)$	1236	1114	1125	225	54
$O(1)H(1)\cdots O(3)$ bend $+ \delta(H_2O)$	992*	1074	1082	251	107
$O=C-O$ bend+ $O(3)H\cdots O=$ out of plane bend	768	731	738	43	12
H_2O libration	686	597	603	179	57
H_2O libration	580	555	560	122	43
CCOOH out of pl. bend	519	469	483	281	90
$\varepsilon_{yy}(\infty) = 1.817$					

The observed frequencies correspond to the maximum reflectance for a particular band and are given here in order to characterize the reflectance bands. These frequencies differ from the transversal one which should appear at lower wavenumbers than the observed one for a pure, non-overlapped reflectance band.

The fitting procedure results in a lower difference between measured and modeled spectrum for the spectrum with polarization direction along the *b* crystallographic axis, then for spectra recorded from the *ac* crystal plane (compare Figs. 4 and 5). Several reasons may be responsible for the poorer fit in the case of spectra recorded from the *ac* crystal plane. The first one may be found in the more complex formula for the dielectric tensor and the reflectance function used in the fitting procedure of the B_u modes, besides, four spectra at different angles of polarization must accommodate the model function. Further, small experimental error could be introduced while rotating the crystal around the *b* crystal axis, although all precautions to exclude this error have been applied. Another, more crucial argument can be found if we scrutinize spectra in Figure 4 more carefully. It can be seen that the fitting fails mostly in the region from 2000 to 1500 cm^{-1}. As already mentioned in earlier

work [11], this is the region where the asymmetric stretching of the strong hydrogen bond appears, and where the strong anharmonic coupling with other modes is expected to be present. Therefore, it is highly probable that this interaction causes an incompatibility with the fitting model, in which such an interaction was not incorporated. Another reason for the poor fit could be also appearance of an Evans hole at a frequency near 1770 cm^{-1}. This kind of Fermi resonance between the stretching C=O and the asymmetric short hydrogen bond stretching has already been detected in the Raman spectra of the compound [11]. However, the model reflectance function does not support this feature. The existence of the Evans hole might be seen on the enlarged section in Figure 6. For comparison, the same section is given for the generated spectra using data from Table 2, for the same angles of polarization. The apparent difference between the experimentally recorded and calculated spectra can be observed.
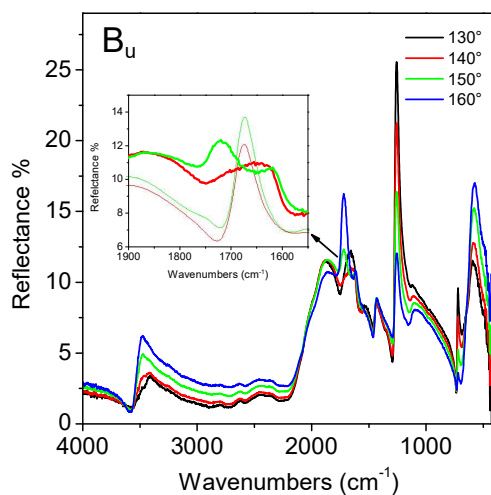
Figure 6. Polarized IR reflectance spectra recorded from the *ac* crystal plane, at $\phi = 130°$, 140°, 150° and 160° (cf. Fig. 1). The insert (pointed by an arrow) shows the enlarged part of the frequency region and the two spectra where the change from a dip, probably with an Evans character, is replaced by a band (bold line). The other two narrow lines are the generated spectra for the 140° and 150° angle of polarization.

When the polarization angle changes from 140° to 150°, it appears that this dip transforms into a band with a maximum at 1717 cm^{-1}, which further shifts to smaller wavenumbers as the polarization angle proceeds to increase. This shift could be explained by the appearance of another band on the low wavenumber side of the first band. Namely the angle between the two calculated transition dipole moments (Table 2) is approximately 52°,

13

which produces the effect of an apparent continuous shift of the reflectance band maximum as polarization angle increases. This kind of continuous shift usually appears between neighboring bands which overlap in a region of several cm^{-1} [15]. The existence of a second band is supported by the fitting results (cf. Table. 2), which were by far worse when only one band was used in the C=O frequency region. It can be also seen that near these two bands exists another small intensity band with maximum reflectance at 1620 cm^{-1} and polarization angle of 150°. This band on the increase of the polarization angle shifts to lower wavenumbers which may be due to the same reason as the previous one, except that in this case it is overlapped with a band at 1541 cm^{-1} and maximum reflectance at 70° of polarization angle.

Nevertheless, the broad reflectance band at 1883 cm^{-1}, appears to possess minimum reflectance at 30° polarization angle, meaning the maximum would be expected near 120°. The reading of the maximum value is however obscured due to the appearance of the strong C=O stretching band nearby. In order to somehow compare the spectroscopic results with the one obtained from the crystal structure determination, we process the data in the following way: From the calculation of the potential energy distribution in the oxalic acid molecule [11] follows that the ν (O-H) is a pure mode. Since the short hydrogen bond is linear [1], (∢ O(1)-H(1)…O(3) = 179.3(6)), the calculated direction of the projection of the O(1)-H(1) distance on the *ac* crystal plane should be close to the direction of the observed (θ = 120°), but also, to the fitted orientation transition moment angle (θ = 132.0°) in that plane. From the calculated angle between the projection of the O(1)-H(1) bond on the *ac* crystal plane given in Table 4, it can be seen that the transition dipole moment of the ν(O-H) mode is oriented closely to the *c* crystallographic axis, which is almost along the *z* axis presented in Figure 1. This is in good agreement with the conclusions made from the Raman experiment measurements [11]. Namely, the O(1)-H(1) bond direction is perpendicular to the *b* crystallographic axis (Table 4), and for polarization vector along the *b* crystal axis, a band due to this mode should not appear (or be very weak), which is consistent with the polarized IR spectrum presented in Figure4; i.e. no broad band around 1900 cm^{-1} is present. This means the observed transition dipole moment direction is close to the direction of the transition moment of the carboxyl O-H stretching as calculated using the structural data from ref. [1].

Table 4. Calculated angles (using the data from ref. [1]) that the O(1)-H(1) direction forms with the *b* crystallographic axis, and the angle between the projection of the O(1)-H(1) direction on the *ac* crystal plane with *a* and *c* crystallographic axes.

∢ (O-H, b)	∢ (O-H$_{(ac)}$, a)	∢ (O-H$_{(ac)}$, c)
89.99°	90.00°	16.32°

The frequency region of water stretching vibrations contains two bands due to the symmetric and asymmetric stretching of water molecules. The characteristic of the polarized spectra is that they appear more or less as single reflectance bands at 80° (max. ref. 3416 cm^{-1}) and 160° (max. ref. 3485 cm^{-1}), (cf. Fig. 7).
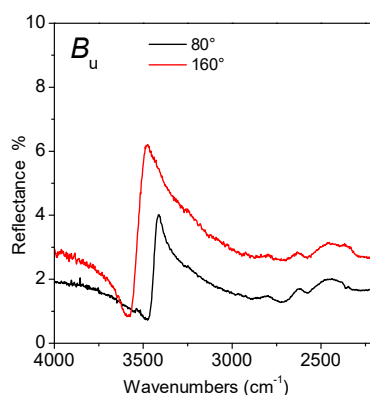
Figure 7. Measured reflectance spectra of the B_u modes, recorded with $\phi = 80°$ and $\phi = 160°$ in the frequency region of water stretching vibration.

The angle between these two dipole moments constitutes 80° (Figure 7). This is of course a rough approximation, because the experimental increment of the polarization angle was 10°. However, it is close to 90°, which is the angle between the symmetric and asymmetric transition dipole moments of a free water molecule. The highly non-mixed character of those normal modes given in ref. [11], confirms this finding.

The next interesting frequency region is the region where coupled ν(C–O) and δ(C–O–H) modes are expected. Two reflectance bands at 1433 (maximum intensity at 150 °) and 1258 cm^{-1} (maximum intensity at 80°), can be found in this region (Figure 8).

15
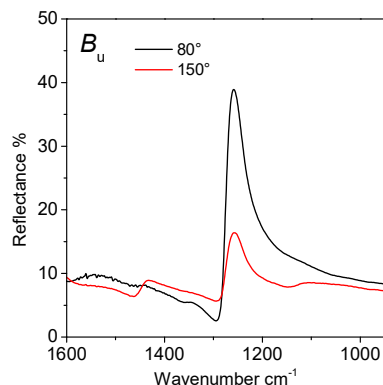
Figure 8. Measured reflectance spectra of the B_u modes, recorded with $\phi = 80°$ and $\phi = 150°$ in the frequency region of the coupled ν(C–O) and δ(C–O–H) modes.

The positions of these two maxima do not change with polarization angle. This implies that these bands are not overlapped with other, comparably strong bands. From the experimental spectra it can be concluded that the angle between their transition dipole moments is approximately 70°, while the result of the fitting is 40°. The characteristic of the band at 1258 cm^{-1} is that its intensity never vanishes completely. This effect is common for the B_u symmetry type modes in monoclinic crystals [22], due to the inability of diagonalization of the dielectric tensor for all of the frequencies (modes) simultaneously.

The reflectance band of the γ(O–H) mode of the B_u symmetry type appears near 1120 cm^{-1}. Due to its expected low intensity it is difficult to find the precise position. This band appears in the vicinity of the strong band at 1258 cm^{-1}. This made the determination of the exact band frequency even more difficult.

The polarized reflection spectra presented in Figure 9 shows that there are two week but sharp bands with maximum frequency difference of about 9 cm^{-1}, whose reflectance maxima appear at polarization angles almost mutually parallel. Both bands are at maximum reflectance or minimum reflectance within 20° difference in the polarization angle.
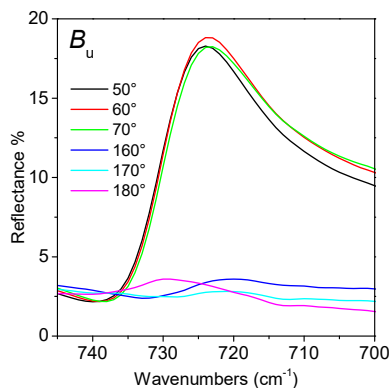
Figure 9. Measured reflectance spectra of the B_u modes, recorded with $\phi = 50º$, $60º$, $70º$, $160º$, $170º$ and $180º$. Depicted are the maxima and the minima of the two bands, together with the intermediate spectra for minimum ($60º$) and maximum ($170º$).

The complete information concerning the IR active modes is gained if the A_u modes are analyzed as well. The fitting is in a good agreement with the experimental spectra and it can be applied for the interpretation of the spectrum. The two stretching modes of water appear in spectrum with polarization along the *b* crystal axis. This is followed by combinations in the frequency region between 3000 cm^{-1} and 1770 cm^{-1}. The stretching C=O mode appears as band with transversal frequency at 1701 cm^{-1} (Table 3), while the δ(O-H) from water molecules appears at 1614 cm^{-1}. The bands due to coupled ν(C–O) + δ(COH) modes that are clearly resolved when polarization is in the *ac* crystal plane, appear as very weak reflectance bands (Figure 3). The reason is that the oxalic acid molecule plane is oriented parallel to the *ac* crystal plane. Therefore, the reflectance due to these two modes is stronger for polarization in the *ac* crystal plane and weaker when the polarization of the electric vector is along the *b* crystal axis.

Quite interesting is the reflection band of the γ(O–H) mode. In the expected region we found two reflection bands with observed frequencies at 1114 cm^{-1} and 1074 cm^{-1}. The later band appears as a shoulder on the low frequency side of a broad band, and is assigned to O(1)H(1)$\cdots$O(3) bend. + δ(H$_2$O) (Table 3). The reflectance of the 1114 cm^{-1} band is in this orientation greater than the reflectance taken from the *ac* plane (Figure 3). This finding is in accordance with the crystal structure; due to the orientation of the oxalic acid plane, the transition dipole moment of the γ(O–H) mode is mostly oriented along the *b* crystallographic axis.

Apart from the polarized IR spectra, a non-polarized reflectance spectrum from a pressed pellet of pure oxalic acid dihydrate was recorded using 6° incidence angle. The experimental spectrum and modeled spectra are presented in Figure 10.
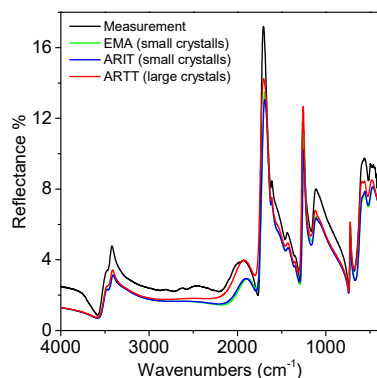
Figure 10. Experimentally recorded reflectance spectra of a polycrystalline pressed pellet α-POX at 6° incidence angle. Modeled reflectance spectra at three different averaging theories obtained by employing single crystal data.

Employing the dielectric tensor elements obtained from the single crystal measurements, it was possible to construct the reflectance spectra of the polycrystalline sample in the frame of EMA (Effective Medium Approximation-small crystallites) [27], ARIT (Average Refractive Index Theory-small crystallites) [28] and ARTT (Average Reflectance and Transmittance Theory-large crystallites) [28, 29].

From the comparison between measured spectrum and modeled spectra it can be concluded that the differences are at a minimum when ARTT theory is employed. This implies that the crystallites (domains) of the oxalic acid obtained by grinding the single crystals in a vibrating mill and consequently pressed in a pellet, possess dimensions larger than the optical resolution of the used electromagnetic radiation which is roughly given by $\lambda/10$ and results at 400 cm^{-1} in a crystallite size of larger than 2.5 microns and decreases to 250 nm at 4000 cm^{-1}.

What is very interesting is that problems with the discrepancies between the modeled and recorded polarized single crystal spectra, previously mentioned, seem not to be present for the polycrystalline phase (the number of bands, their frequencies and shape are the same). This effect is probably due to the averaging. It has to be kept in mind that actually the modeled polycrystalline spectra are obtained using the data previously gained from the single crystal investigations, which at least for the ac crystal face appeared not to be quite satisfactory, but are nevertheless confirmed by the good overall agreement of band shapes,

18

peak positions and relative peak intensities [28]. It can be concluded that the reasons for the ambiguous fitting result of the polarized single crystal spectra are of the small scale and directionally dependent. Thus, these effects can be exclusively investigated by applying the single crystal specimen.

6. Conclusions

The presented series of polarized spectra of α−oxalic acid dihydrate, allowed the differentiation between A_u and B_u symmetry type modes. All four water stretching modes (two of A_u and two of B_u symmetry) were identified. In order for the fit to give better results, extra oscillators around 3369 cm^{-1} and 3299 cm^{-1} should have to be included. The origin of those oscillators is obscured by the existence of the strong and wide O-H carboxyl stretching band. Therefore, it is not clear whether those bands are a part of the wide band flank or have a different source. The comparison of the spectroscopic results with the structural data suggests that the band with transversal frequency at 1881 cm^{-1} (fitted value) originates from the O–H carboxyl stretching. The unsatisfying fit, particularly in the frequency region where the bands of the O-H carboxyl stretching and the C=O modes appear is ascribed to the possible presence of the Evans type of interaction and strong anharmonicity of the OH stretching band. If the Evans hole is present that also implies that the band maxima of strong O-H…O hydrogen bond is not at 1881 cm^{-1} but significantly lower close to the 1600 cm^{-1}.

The maxima of the reflectance bands of the coupled ν(C–O) and δ(C–O–H) do not change with polarization, since they do not overlap with other bands. The intensity of these bands is large for the spectrum recorded from the *ac* crystal plane, and negligible for a polarization along the *b* crystal axis, which is consistent with structural data. Due to the planarity of the oxalic acid molecule, that is almost parallel to the *ac* crystal plane, the γ(O–H) mode will have a transition dipole moment close to the direction of the *b* crystallographic axis. This is consistent with the results of our experiments, where the γ(O–H) band readily appears at 1125 cm^{-1} for the *b* polarization and has very low intensity for the *ac* polarization. The remaining deviations between simulations and measurements in the reflectance spectra recorded from the *ac* crystal plane, can probably be removed by the employment of reflectance models with inclusion of the interaction between neighboring modes [30] or inclusion of Evans type of interaction between the modes [31].

The modeled polycrystalline non-polarized IR spectrum assuming large crystallites resembles the actually recorded IR spectrum comparably well. The differences that existed in some particular spectral regions between the modeled and the recorded single crystal spectra are

absent when polycrystalline samples were used. The averaging takes into account all the directions. Thus, it follows that the effects due to which the ambiguous single crystal fitting result appeared, are probably directionally defined.

7. References

[1] T.M. Sabine, G.W. Cox, B.M. Craven, A neutron diffraction study of [alpha]-oxalic acid dihydrate, Acta Crystallographica Section B 25(12) (1969) 2437-2441.
[2] R.G. Delaplane, J.A. Ibers, An X-ray study of [alpha]-oxalic acid dihydrate (COOH)2.2H2O and of its deuterium analogue, (COOD)2.2D2O: isotope effect in hydrogen bonding and anisotropic extinction effects, Acta Crystallographica Section B 25(12) (1969) 2423-2437.
[3] L. Zheng, K.W. Fishbein, R.G. Griffin, J. Herzfeld, Two-dimensional solid-state proton NMR and proton exchange, Journal of the American Chemical Society 115(14) (1993) 6254-6261.
[4] A. Levstik, C. Filipič, V. Bobnar, I. Levstik, D. Hadži, Polaron conductivity mechanism in oxalic acid dihydrate: ac conductivity experiment, Physical Review B 74(15) (2006) 153104.
[5] V. Mohaček-Grošev, J. Grdadolnik, D. Hadži, Evidence of Polaron Excitations in Low Temperature Raman Spectra of Oxalic Acid Dihydrate, The Journal of Physical Chemistry A 120(18) (2016) 2789-2796.
[6] S.W. Johnson, M. Barthes, J. Eckert, R.K. McMullan, M. Muller, Comment on ``Dynamical Test of Davydov-Type Solitons in Acetanilide Using a Picosecond Free-Electron Laser'', Physical Review Letters 74(14) (1995) 2844-2844.
[7] P. Hamm, J. Edler, Quantum vibrational polarons: Crystalline acetanilide revisited, Physical Review B 73(9) (2006) 094302.

[8] F.F. Iwasaki, H. Iwasaki, Y. Saito, The crystal structure of deuterated oxalic acid dihydrate (COOD)2.2D2O, by neutron diffraction analysis, Acta Crystallographica 23(1) (1967) 64-70.

[9] P. Coppens, T.M. Sabine, Neutron diffraction study of hydrogen bonding and thermal motion in deuterated [alpha] and [beta] oxalic acid dihydrate, Acta Crystallographica Section B 25(12) (1969) 2442-2451.

[10] L.J. Bellamy, R.J. Pace, Hydrogen bonding in carboxylic acids—I. Oxalic acids, Spectrochimica Acta 19(2) (1963) 435-442.

[11] V. Mohaček-Grošev, J. Grdadolnik, J. Stare, D. Hadži, Identification of hydrogen bond modes in polarized Raman spectra of single crystals of α-oxalic acid dihydrate, Journal of Raman Spectroscopy 40(11) (2009) 1605-1614.

[12] M.D. King, T.M. Korter, Effect of Waters of Crystallization on Terahertz Spectra: Anhydrous Oxalic Acid and Its Dihydrate, The Journal of Physical Chemistry A 114(26) (2010) 7127-7138.

[13] M. Belousov, V. Pavinich, Infrared reflection spectra of monoclinic crystals, Optics and Spectroscopy 45 (1978) 771-774.

[14] J.R. Aronson, A.G. Emslie, E.V. Miseo, E.M. Smith, P.F. Strong, Optical constants of monoclinic anisotropic crystals: gypsum, Appl. Opt. 22(24) (1983) 4093-4098.

[15] V. Ivanovski, T.G. Mayerhöfer, J. Popp, Investigation of the peculiarities in the polarized reflectance spectra of some Tutton salt monoclinic single crystals using dispersion analysis, Vibrational Spectroscopy 44(2) (2007) 369-374.

[16] V. Ivanovski, T.G. Mayerhöfer, J. Popp, V.M. Petruševski, Polarized IR reflectance spectra of the monoclinic single crystal K2Ni(SO4)2·6H2O: Dispersion analysis, dielectric and optical properties, Spectrochimica Acta Part A: Molecular and Biomolecular Spectroscopy 69(2) (2008) 629-641.

[17] V. Ivanovski, T.G. Mayerhöfer, J. Popp, Dispersion analysis of polarized IR reflectance spectra of Tutton salts: The ν3(SO42−) frequency region, Vibrational Spectroscopy 47(2) (2008) 91-98.

[18] M. Boero, A. Curioni, J. Hutter, A. Isayev, A. Kohlmeyer, N. Nair, W. Quester, Ł. Walewski, Car–Parrinello Molecular Dynamics, 1990–2008, Google Scholar.

[19] N. Troullier, J.L. Martins, Efficient pseudopotentials for plane-wave calculations, Physical Review B 43(3) (1991) 1993-2006.

[20] M. Born, E. Wolf, Principles of Optics: Electromagnetic Theory of Propagation, Interference and Diffraction of Light, Cambridge University Press, Cambridge, 2006.

[21] R.L. Redington, T.E. Redington, Infrared matrix-isolation spectra of monomeric oxalic acid, Journal of Molecular Structure 48(2) (1978) 165-176.

[22] J. Nieminen, M. Rasanen, J. Murto, Matrix-isolation and ab initio studies of oxalic acid, The Journal of Physical Chemistry 96(13) (1992) 5303-5308.

[23] V. Ivanovski, T.G. Mayerhöfer, J. Popp, Isosbestic-like point in the polarized reflectance spectra of monoclinic crystals—A quantitative approach, Spectrochimica Acta Part A: Molecular and Biomolecular Spectroscopy 68(3) (2007) 632-638.

[24] V. Ivanovski, T.G. Mayerhofer, Vibrational spectra and dispersion analysis of K2Ni(SeO4)2.6H2O Tutton salt single crystal doped with K2Ni(SO4)2.6H2O, Spectrochimica acta. Part A, Molecular and biomolecular spectroscopy 114 (2013) 553-62.

[25] M.K. Gunde, V. Ivanovski, B. Orel, Dispersion Analysis of Polarized Bulk Reflectance Spectra of Potassium Hydrogen Succinate Monocrystal, Acta Chimica Slovenica 58(3) (2011) 528-541.

[26] T.G. Mayerhöfer, V. Ivanovski, J. Popp, Dispersion analysis of non-normal reflection spectra from monoclinic crystals, Vibrational Spectroscopy 63 (2012) 396-403.

[27] C. Pecharromán, J.E. Iglesias, Effective dielectric properties of packed mixtures of insulator particles, Physical Review B 49(11) (1994) 7137-7147.

[28] T.G. Mayerhöfer, J. Popp, Employing spectra of polycrystalline materials for the verification of optical constants obtained from corresponding low-symmetry single crystals, Appl. Opt. 46(3) (2007) 327-334.

[29] T.G. Mayerhöfer, Modelling IR-spectra of single-phase polycrystalline materials with random orientation—a unified approach, Vibrational Spectroscopy 35(1-2) (2004) 67-76.

[30] V. Ivanovski, G. Ivanovski, Nearest-neighbour-interaction model in the coupled-optical-phonon-mode theory of the infrared dispersion in monoclinic crystals: Application to Tutton salt single crystal, Spectrochimica Acta Part A: Molecular and Biomolecular Spectroscopy 75(5) (2010) 1452-1461.

[31] P. Kondratyuk, Analytical formulas for Fermi resonance interactions in continuous distributions of states, Spectrochimica Acta Part A: Molecular and Biomolecular Spectroscopy 61(4) (2005) 589-593.